Supporting Information

Dependency of Sliding Friction for Two Dimensional Systems on Electronegativity

Jianjun Wang[a,b,d], Avinash Tiwari[d], Yang Huang [b], Yu Jia[b, c,*], Bo N. J. Persson[d]

[a] *College of Science, Zhongyuan University of Technology, Zhengzhou, Henan 450007, China*

[b]*Key Laboratory for Special Functional Materials of Ministry of Education, and School of Materials Science and Engineering, Henan University, Kaifeng, Henan 475004, China*

[c]*International Laboratory for Quantum Functional Materials of Henan, and School of Physics, Zhengzhou University, Zhengzhou, Henan 450001, China*

[d]*PGI-1, FZ-Juelich, Germany, EU*

[*] jiayu@zzu.edu.cn (Y Jia)

1. Tables

Table S1

Table S1. Energies of symmetric stacking of graphene/graphene (equilibrium interlayer distance d_{eq} and optimal binding energy E_{AB} in AB stacking; the magnitude of corrugation of the PES $\Delta E_{AA} = E_{AA} - E_{AB}$, the magnitude of the saddle point in the PES $\Delta E_{SP} = E_{SP} - E_{AB}$). The reference numbers listed are the same as those in the revised manuscript.

Approach	d_{eq} (Å)	E_{AB} (meV/atom)	ΔE_{AA} (meV/atom)	ΔE_{SP} (meV/atom)	Reference
PBE-MBD, relaxed	3.423	-46.39	6.99	0.89	This work
PBE-MBD, relaxed	3.37	-45.6	8	~1	Ref. [16]
PBE-MBD, fixed to 3.4 Å	3.423	-46.39	12.47	1.39	This work
PBE-MBD, fixed to 3.4 Å	3.423	-45.26	12.34	1.38	Ref. [33]
PBE-MBD, fixed to 3.37 Å	3.37	-45.6	10.8	~1.2	Ref. [16]
PBE-D2, fixed to 3.26 Å	3.256	-50.41	19.20	2.04	Ref. [34]
PBE-D2, fixed to 3.4 Å	3.248	-49.68	20.7	2.32	Ref. [33]
PBE-D3, fixed to 3.4 Å	3.527	-42.8	7.6	0.84	Ref. [33]
PBE-TS, fixed to 3.36 Å	3.36	-73.05	15.3	1.88	Ref. [34]
PBE-TS, fixed to 3.4 Å	3.367	-72.72	15.94	2.02	Ref. [33]
Exp.			15.4	1.71	Refs. [35, 36]
Exp. (graphite)	3.34				Ref. [37]
Exp. (graphite)		52±5			Ref. [38]

Table S2

Table S2. Energies of symmetric stacking of *h*-BN/*h*-BN (equilibrium interlayer distance in *AA′* stacking d_{eq}, binding energy in *AA′* stacking $E'_{AA'}$, the magnitude of corrugation of the PES $\Delta E'_{A'B} = E'_{A'B} - E'_{AA'}$, (*A′B* is the highest energy stacking, staggered with N over N atoms) the magnitude of the saddle point of the PES $\Delta E'_{sp} = E'_{sp} - E'_{AA'}$). The reference numbers listed are the same as those in the revised manuscript.

Approach	d_{eq} (Å)	$E'_{AA'}$ (meV/atom)	$\Delta E'_{A'B}$ (meV/atom)	$\Delta E'_{sp}$ (meV/atom)	Reference
PBE-MBD, relaxed	3.33	-54.54	10.11	1.97	This work
PBE-MBD, relaxed	3.37	-49.6	9.7	~2	Ref. [16]
PBE-MBD, fixed to 3.33 Å	3.33	-54.54	14.41	2.3	This work
PBE-MBD, fixed to 3.37 Å	3.37	-49.6	14.7	~2.5	Ref. [16]
PBE-D2, fixed to 3.12 Å	3.12	-68.77	26.86	4.7	Ref. [34]
PBE-D3, fixed to 3.348 Å	3.438	-44.04	10.82	2.5	Ref. [34]
PBE-TS, fixed to 3.368 Å	3.368	-75.89	10.61	0.98	Ref. [34]
Exp.(10 Layers)	3.25±0.1				Ref. [39]

2. Figures

Figure S1

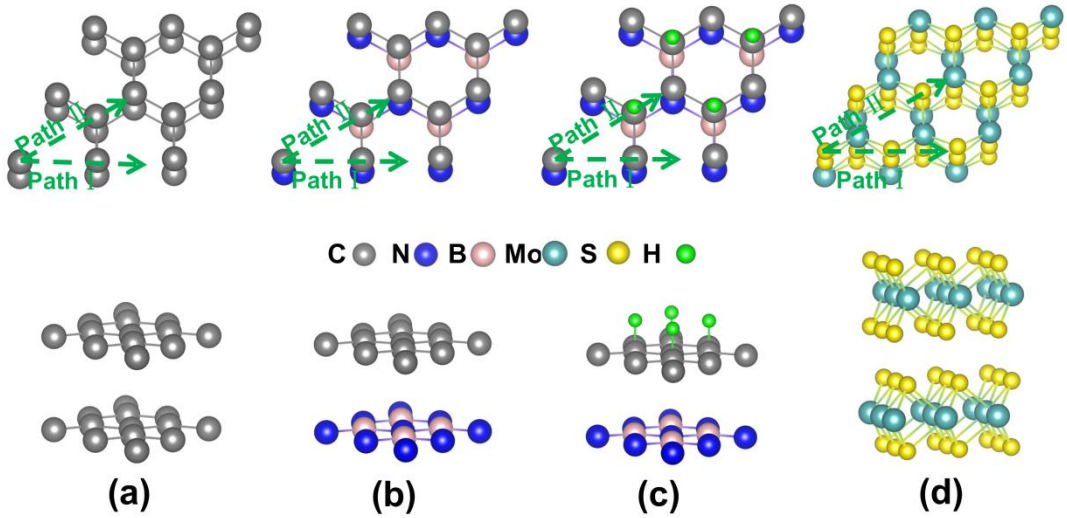

Fig. S1. The sliding models for (a) graphene/graphene, (b) graphene/*h*-BN, (c) H-graphene/*h*-BN and (d) MoS_2/MoS_2. The upper and bottom planes are top and side views of bilayer sliding systems, respectively.

Figure S2

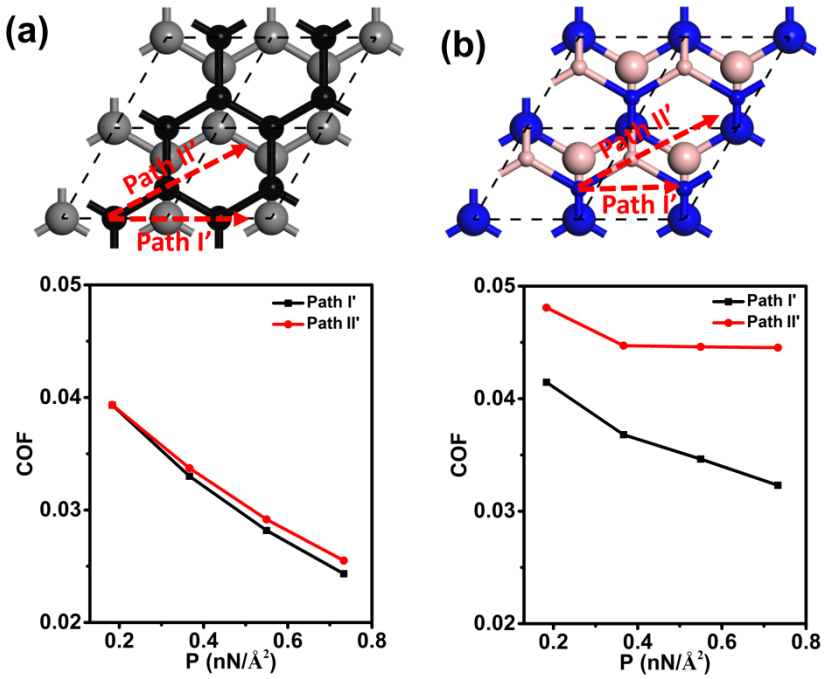

Fig. S2. The structures and friction for (a) graphene/graphene and (b) *h*-BN/*h*-BN systems along two paths with small friction. By moving the two sheets relative to each other by half a bond length, two other small barrier sliding paths were construct. Although the friction and polarity are significantly reduced, the friction difference between the polar and non-polar systems is noticeable.

Figure S3

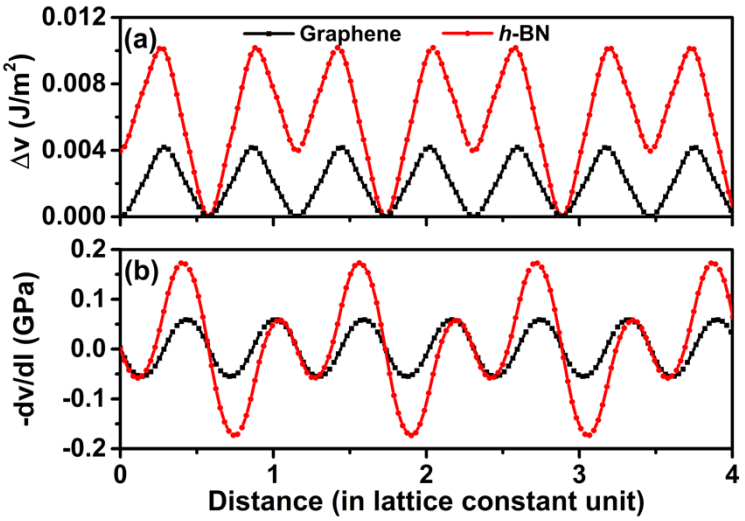

Fig. S3. The comparison of (a) potential barriers and (b) friction forces per unit area along minimum potential energy paths (zigzag path) between graphene/graphene and *h*-BN/*h*-BN systems. The magnitude of barrier in the polar *h*-BN/*h*-BN system is twice that of the graphene/graphene system, and there is a saddle point between two minimum points in the *h*-BN/*h*-BN system.

Figure S4

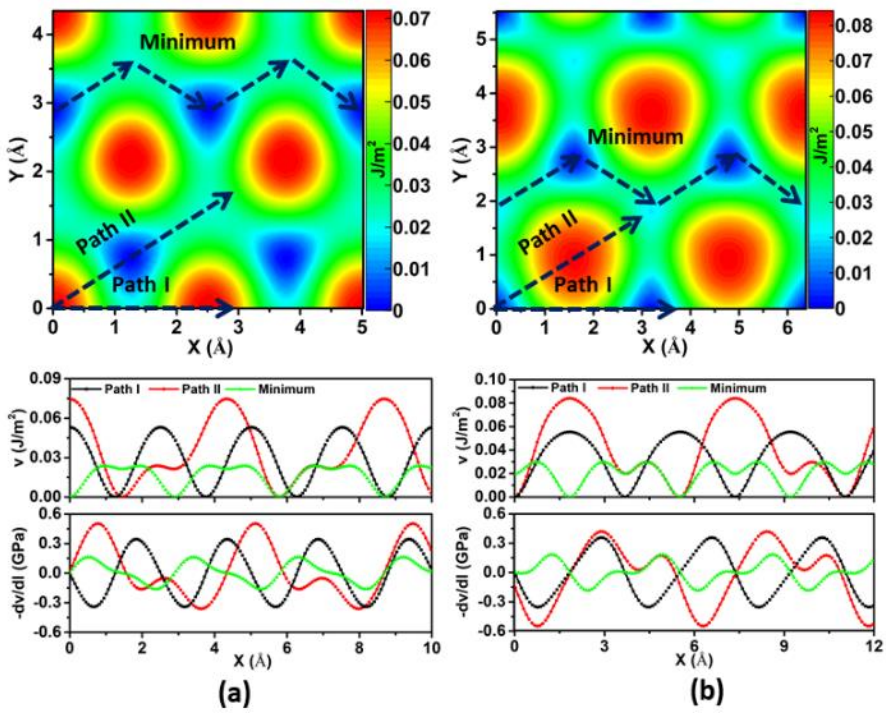

Fig. S4. The potential energy surfaces of (a) H-graphene/*h*-BN and (b) MoS_2/MoS_2 systems. The absolute PES minimum is taken as a reference. The corresponding potential barriers and friction forces per unit area along the three chosen paths are plotted under each PES.

Figure S5

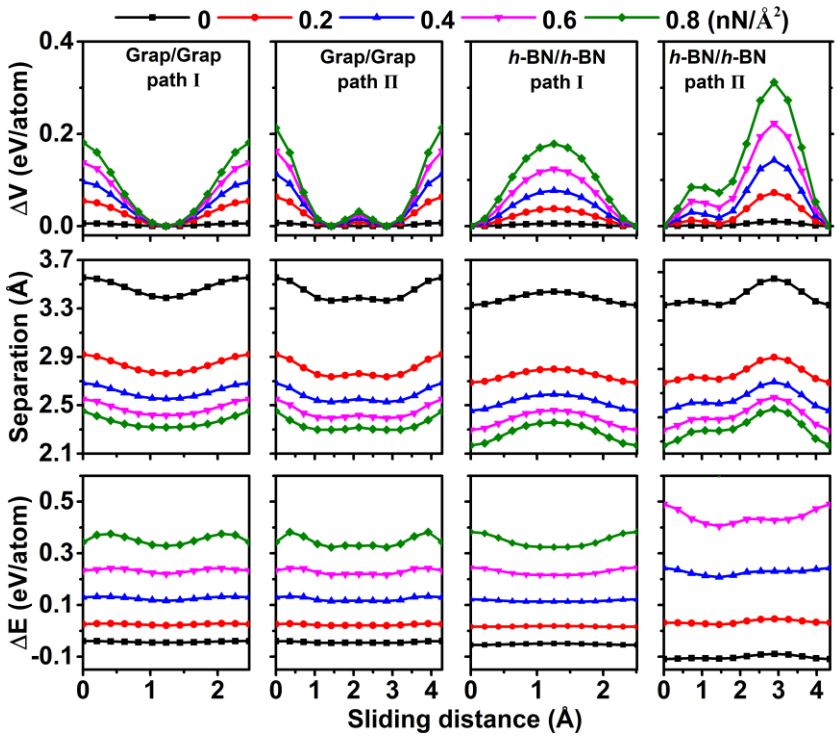

Fig. S5. Sliding barrier ΔV, interlayer separation, and binding energy ΔE as a function of sliding distance for graphene/graphene and *h*-BN/*h*-BN systems along path I and II, respectively.

Figure S6

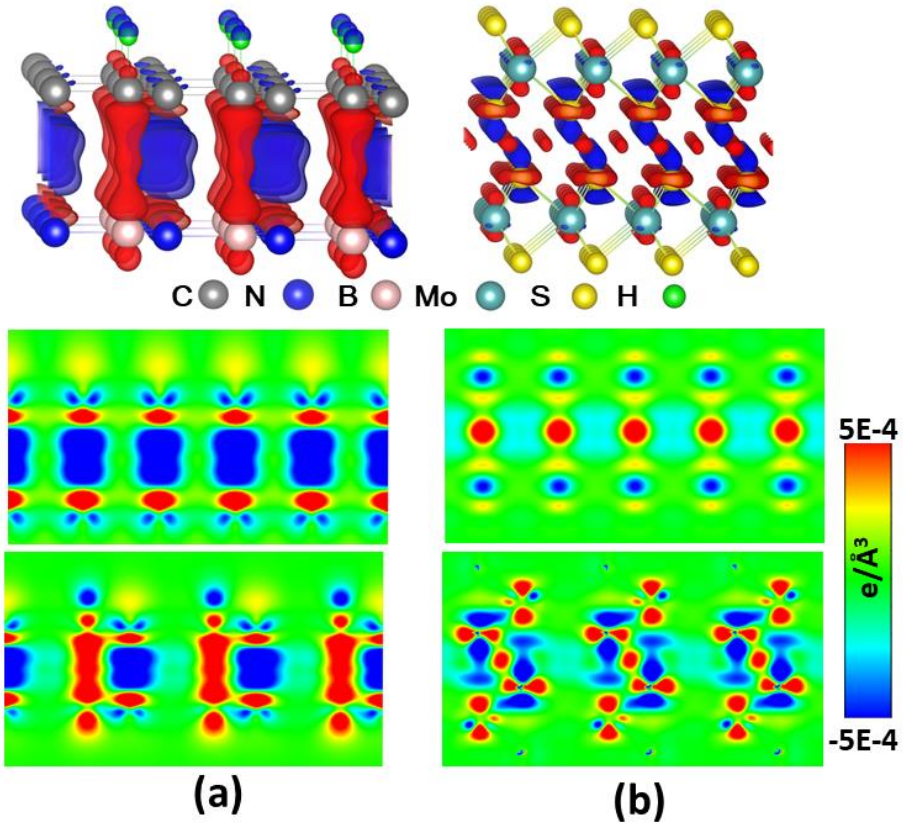

Fig. S6. The charge density difference of (a) H-graphene/*h*-BN and (b) MoS_2/MoS_2 systems, respectively. Red and blue indicating charge accumulation and depletion regions, and the isosurface charge density is taken as 0.0005 electrons/Å^3. Middle and bottom planes are the charge density differences along paths I and II shown in Fig. S1.